

Finite Element Analysis of Impact Damaged Honeycomb Sandwich

D.P.W. Horrigan and R.R Aitken

Centre for Polymer and Composites Research, Department of Mechanical Engineering, The University of Auckland, Private Bag 92019, Auckland, New Zealand.

Abstract

Due to high stiffness and strength to weight ratios, composite sandwich is used increasingly in aerospace applications. The main drawback of sandwich structure is its low resistance to impact damage and the extent to which the strength of the structure is reduced under compressive loading. In this study, it is proposed that a continuum damage model is used to model crushing due to impact. The model describes the compressive behaviour of honeycombs made from materials that are prone to elastic buckling. The material behaviour in compression is described by a combination of three constitutive models namely elastic, continuum damage and inelastic strain accumulation. The model has been interfaced with LUSAS and is used to model “soft” impacts onto minimum gauge Nomex™ sandwich. The materials and dimensions are typical of sandwich panels found in commercial aircraft. Results from analysis are compared to experimental data and are found to compare well. The outcome is the ability to evaluate impact damage for various honeycomb sandwiches.

Introduction

Composite sandwich construction is becoming more common in aircraft structure. This is essentially because such panels offer high stiffness to weight and, in some cases, also the best strength to weight ratios. However, sandwiches are generally poor at resisting impact damage. Impact may come from a variety of causes. Typically, low speed impacts may result from tool drops, hail and debris thrown up from runways. In the literature, these types of impact have received a great deal of attention [1,2,3] for good reasons. They are a common form of damage and present an easy case to simulate analytically and experimentally. Typically, experimental data is generated using a steel ball indenter to create the damage zone. This creates a high mass - low speed impact. However, sandwich panels

also suffer impacts from high speed - low mass bodies such as birds. Typical examples are the trailing-edge wedges of aircraft flaps. Soft bodies are highly deformable compared to rigid ball indentors and do not create the same distribution of damage in the core [4]. Consequently, the aim of this research is to develop a model to simulate a range of impacts onto sandwich panels.

Metal honeycombs such as Aluminium deform by *plastic* buckling and are commonly well modelled as elastic, perfectly-plastic materials. In comparison, materials made from random, short fibres embedded in an epoxy matrix tend to fail predominantly by *elastic* buckling under compressive loading. After buckling, the core does not recover its original buckling strength due to local damage to the short fibres at the kinks and the altered geometry of the cells. The kinks become permanent “hinges” left in the core material. As a result, these cores are left in a state where the hinges deform from the start of load application. The core then appears to deform elastically but with a reduced stiffness. Core damage due to soft body impact is shown in Figure 1.

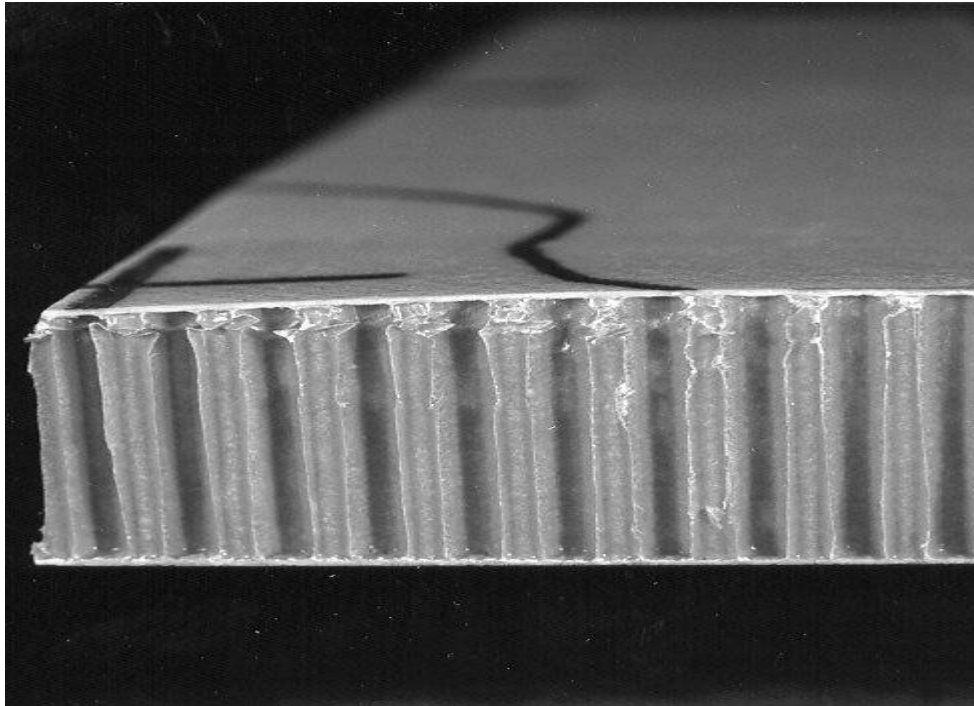


Figure 1 - Honeycomb crushing due to a deformable body impact.

The difference between a hard and soft impact is interesting. Figure 2 shows an impact where a rigid ball was used. The damage is a parabolic shaped region, with the maximum depth at the centre. The damage after impact by a deformable body has a depth of damage across the defect that is uniform. Clearly, damage due to a deformable or “*soft*” body does not create the same profile as a hard body.

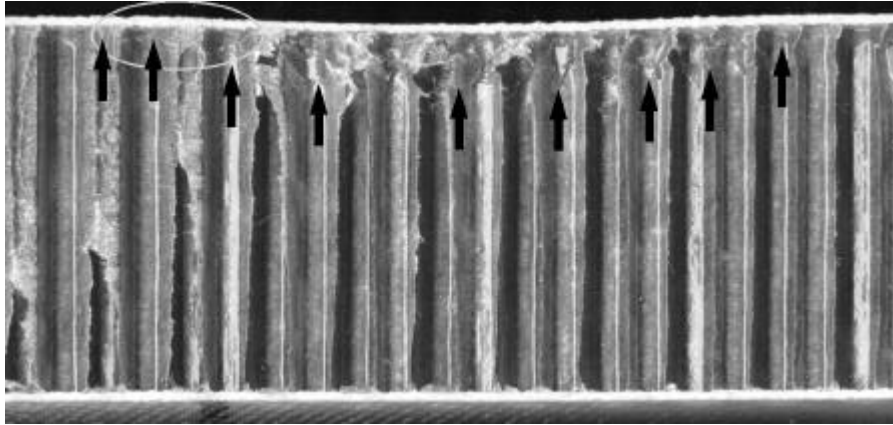


Figure 2 - Experimental rigid body impact.

Accordingly, the aim of this work is to develop a method by which impact damage can be modelled using finite element analysis. It should be valid for both soft and hard impacts.

Core Behaviour.

Previous studies of compressive failure in metal honeycomb [10] has shown that the overall response is generally similar to that of an elastic-perfectly plastic material, especially where the material exhibits lower levels of strain hardening. When the material buckles locally, plastic hinges form and it is here that the bulk of the real inelastic strains are accumulated. On unloading, the small elastic strains are recovered from the plastic material in the neighbourhood of the hinges.

In contrast, impacts with a material such as Nomex™ exhibit more complex behaviour both on loading and unloading. The initial buckling of the core is elastic in nature. As a result, the formation of hinges in the core material decreases its stiffness rapidly due to the geometrical changes that have occurred. The force sustained in the damaged material falls accordingly.

Figure 3 shows a typical plot of the nominal stress-strain behaviour for a Nomex™ sample under *quasi-static* through-thickness compression. From a mechanical perspective the most notable difference between non-metallic and metallic honeycomb structure is the post buckling load carrying capacity. Non-metallic honeycomb loses a large proportion of its stiffness post-buckling. In contrast, metallic honeycomb retains significant load carrying capacity because further deformation requires additional plastic work.

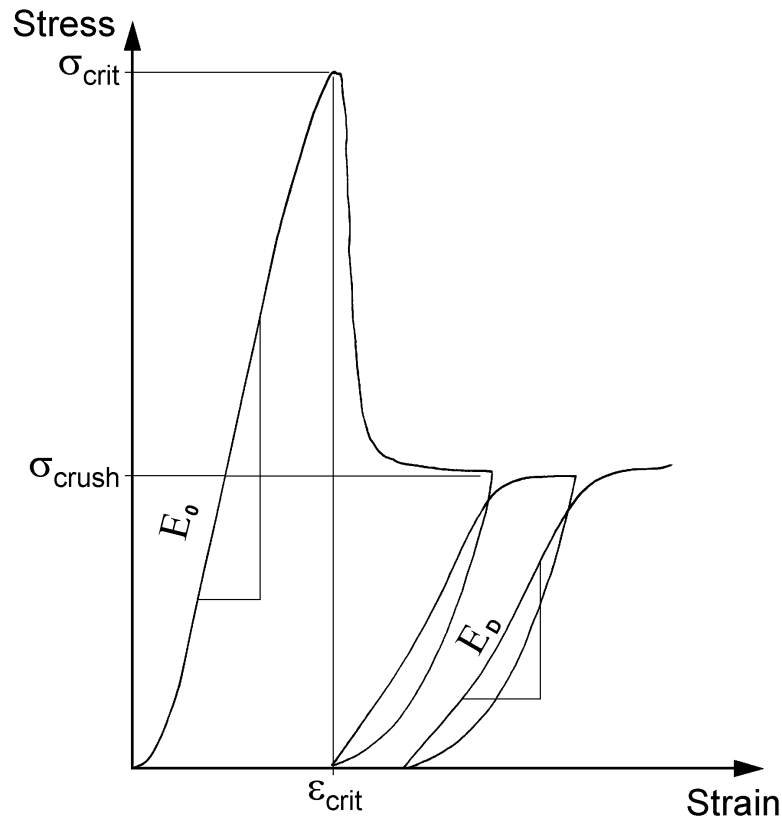


Figure 3 - Nominal Stress-Strain behaviour of Nomex™ core

The fall in this curve represents a decrease in the strain energy as the material buckles. Physically, the material forms a number of local wrinkle sites and begins to deform in a concertina fashion. The material between the wrinkles stores much less elastic energy than the small volume associated with the wrinkles stores a combination of elastic and inelastic energy. Subsequent to the initial buckling, the material exhibits steady crushing. The loading history shown in Figure 3 can be divided into three regions as follows:

1. Elastic loading to the point where the critical stress, σ_{crit} is reached.
2. Rapid decrease in the apparent stiffness of the core material.
3. Steady crushing, during which inelastic strains accumulate.

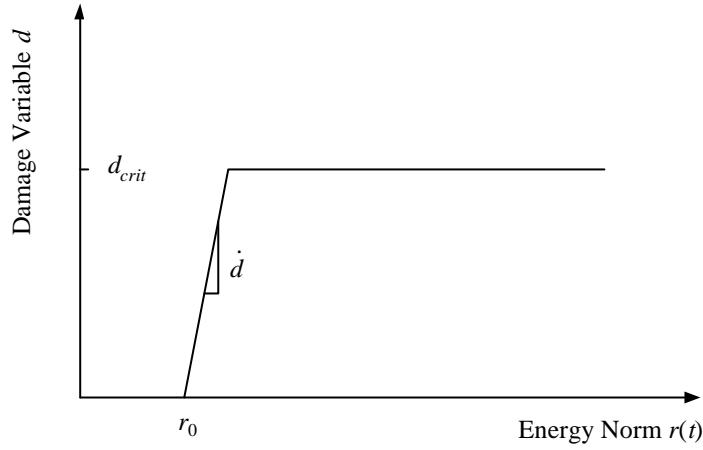


Figure 4 – Damage Evolution.

During elastic loading, the honeycomb is modelled as an orthotropic solid to account for the large variation in its stiffness in its principal directions. This is valid until the peak stress \mathbf{s}_{crit} is attained. An elastic continuum damage model is used to create the apparent change in stiffness (geometry) of the honeycomb. The main requirements of the damage evolution are that the decrease in stiffness occurs as rapidly as possible and that it causes the same reduction as the experimental samples. This has been achieved in LUSAS with a modified user defined damage potential function. A schematic of this damage function is shown in Figure 4.

Considering Figure 3, it is clear that buckling happens very rapidly. The change in the stress-strain curve occurs approximately at a fixed strain, \mathbf{e}_{crit} . This is verified experimentally even at low strain rates. Under this assumption and the dominant through thickness elastic properties, the following relationship is developed:

$$\mathbf{e}_{crit} = \frac{\mathbf{s}_{crit}}{E_0} \approx \frac{\mathbf{s}_{crush}}{E_D} \quad (1)$$

Rearranging equation (1), approximate ratio equivalence between the critical stresses and moduli is found (2). The stress ratio is related to the damage multiplier, giving:

$$\frac{E_D}{E_0} = \frac{\mathbf{s}_{crush}}{\mathbf{s}_{crit}} = 1 - d_{max} \quad (2)$$

From experimental data, the reduction in stiffness was found to be 60% for typical Nomex honeycomb, giving a modulus ratio of 40%. Subsequent to the reduction in stiffness achieved by the damage accumulation, any further load application should result in steady crushing similar to an elastic, perfectly-plastic material. For a static loading case this would be hard to model using a yield surface criterion.

The rapid rise in load during an impact event means that the behaviour shown in Figure 3 is suppressed. Under these conditions, although the stress in the material is trying to fall, the externally applied load rises more rapidly. Consequently, instead of the behaviour in Figure 3, under impact conditions the stress level increases until steady crushing occurs. As a result, the damage evolution and the start of the inelastic strains probably start at about the same time. If the damage gradient is sufficiently high, the damage event is completed rapidly and any subsequent increase in load will simply add to the inelastic strain component.

To illustrate this, a model of a honeycomb specimen was impacted with damage properties and the modified evolution law but without any inelastic behaviour. Figure 5 shows that the stress level is indeed increasing under the rapid load application. In contrast, a quasi-static model allows the stress to start falling.

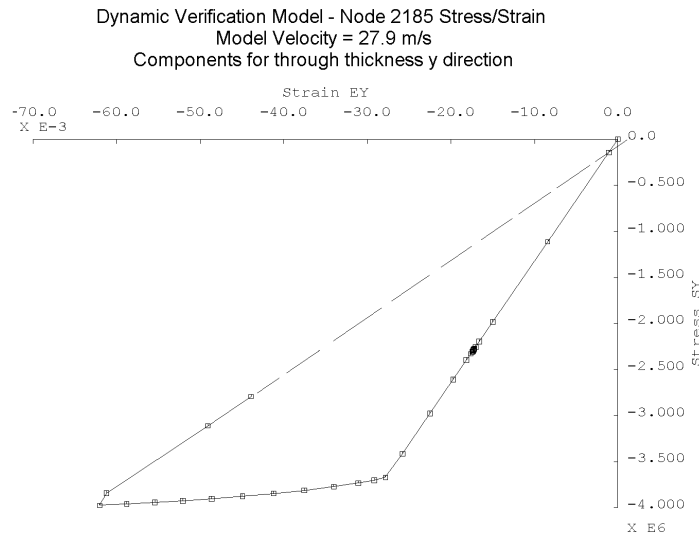


Figure 5 – Impact response of honeycomb with the damage model.

The application the plasticity model post buckling is appropriate for modelling impact with small levels of indentation only. Large levels of indentation may not be modelled well because the plasticity model permits flow that is not characteristic of a crushing honeycomb resulting in excess flow in the ribbon and transverse directions.

The isotropic model allows damage to occur under both tensile and compressive loading. Since buckling occurs at much lower load levels compared to tensile failure and to avoid tensile damage progression, the model modified so that damage may only develop under compression. Damage may only occur when the hydrostatic stress less than zero:

$$\sum_{i=1,3} s_{ii} < 0 \quad (3)$$

Under these conditions there is a net compressive state and damage is permitted to progress accordingly.

Numerical Simulation

Two different numerical simulations have been performed. The first is a soft impact event while the second replaces the soft projectile with a smaller, rigid impactor. This allows a comparative analysis of the proposed continuum damage model under conditions of both soft and hard impact types.

The model uses axisymmetric, explicit dynamic elements with Eulerian geometric non-linearity. Slidelines are used in the model not only to account for the contact between the impacting body and the sandwich but also to tie components of the sandwich model together. The finite element mesh is displayed in Figure 6.

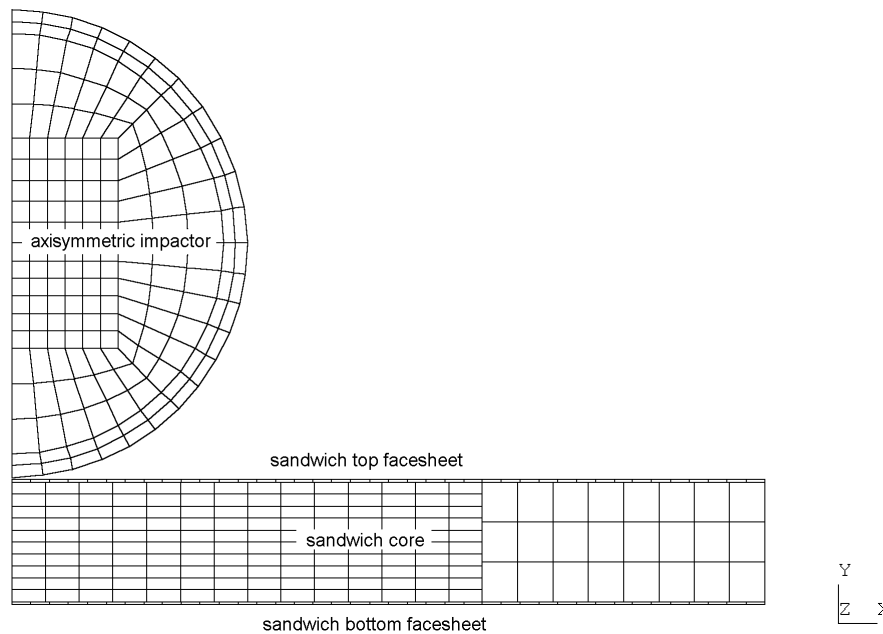


Figure 6 - Finite element model.

For the experiments the impactor was a rubber membrane filled with water. For modelling purposes, the incompressible fluid was modelled as an isotropic, elastic material with a low Young's modulus and a Poisson's ratio close to 0.5 to allow constant volume deformation.

Supports were placed along the panel boundary to constrain the outer edge of the target in a similar fashion to the clamps used in the experimental program. For both the soft and rigid body impacts the projectile is loaded with an initial velocity in the -y direction. After the initial time step the projectile is permitted to decelerate and deform as required by the contact. In both cases the projectile motion is normal to the target surface. This is in contrast to the experimental impacts where the impacts have an incidence angle. For comparative purposes the normal velocity component of experimental results is used for the numerical simulations.

The continuum damage model requires three values to be input. The first is the damage threshold, the critical value of the complementary for damage development. The second is the gradient of the damage function and the last the maximum permissible value of damage (d_{max}). The values used for both analyses are in Table 1.

Damage Parameter	Value
Damage threshold, r_0	320
Damage function gradient, \dot{d}	0.2
Maximum damage value, d_{max}	0.6

Table 1 - Honeycomb continuum damage model parameters.

The numerical simulation of the soft impact event is outlined in Figure 7. The figure contains eight snapshots of the deformed mesh over a total elapsed time of about 4.7ms.

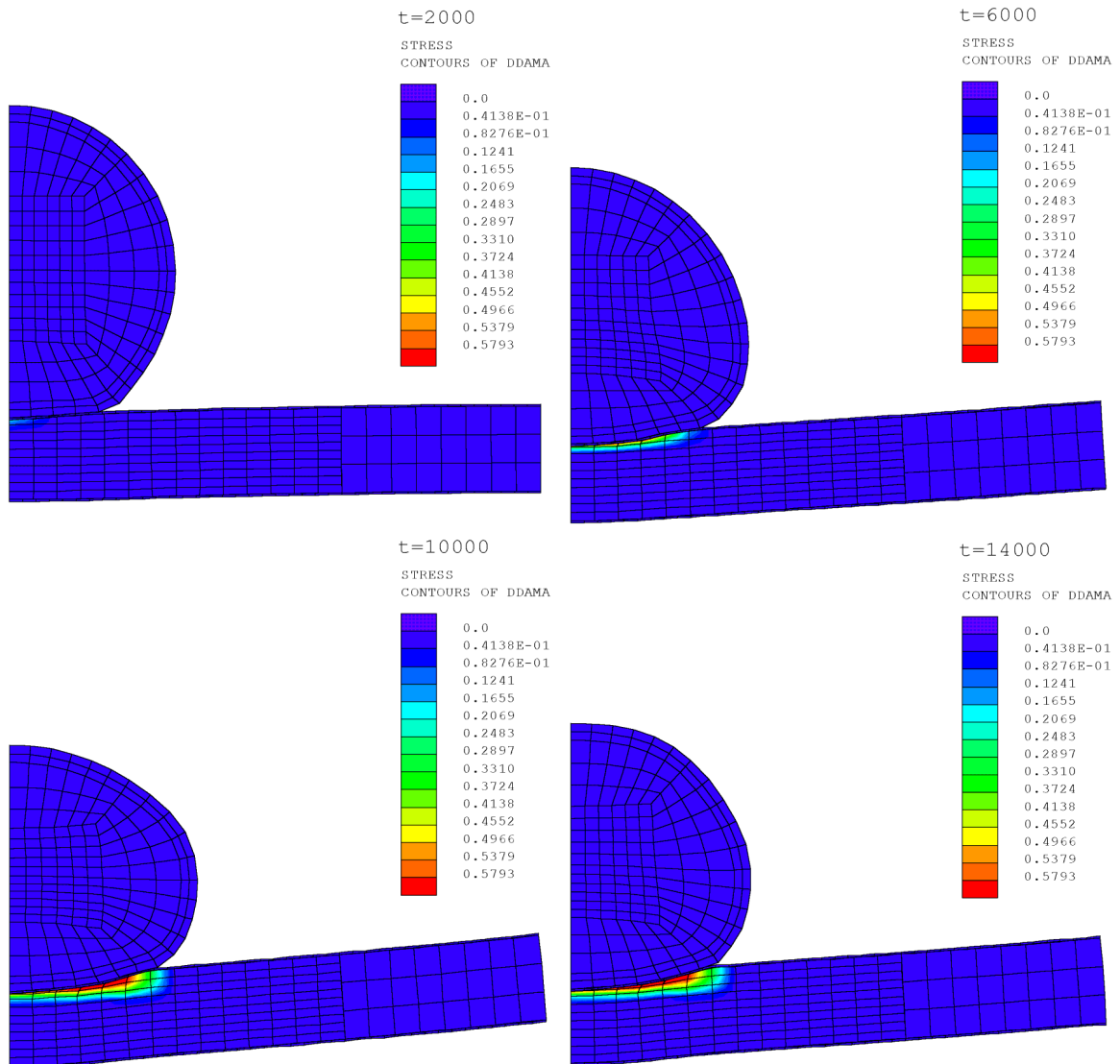


Figure 7a - Soft impact model response steps 1 to 4

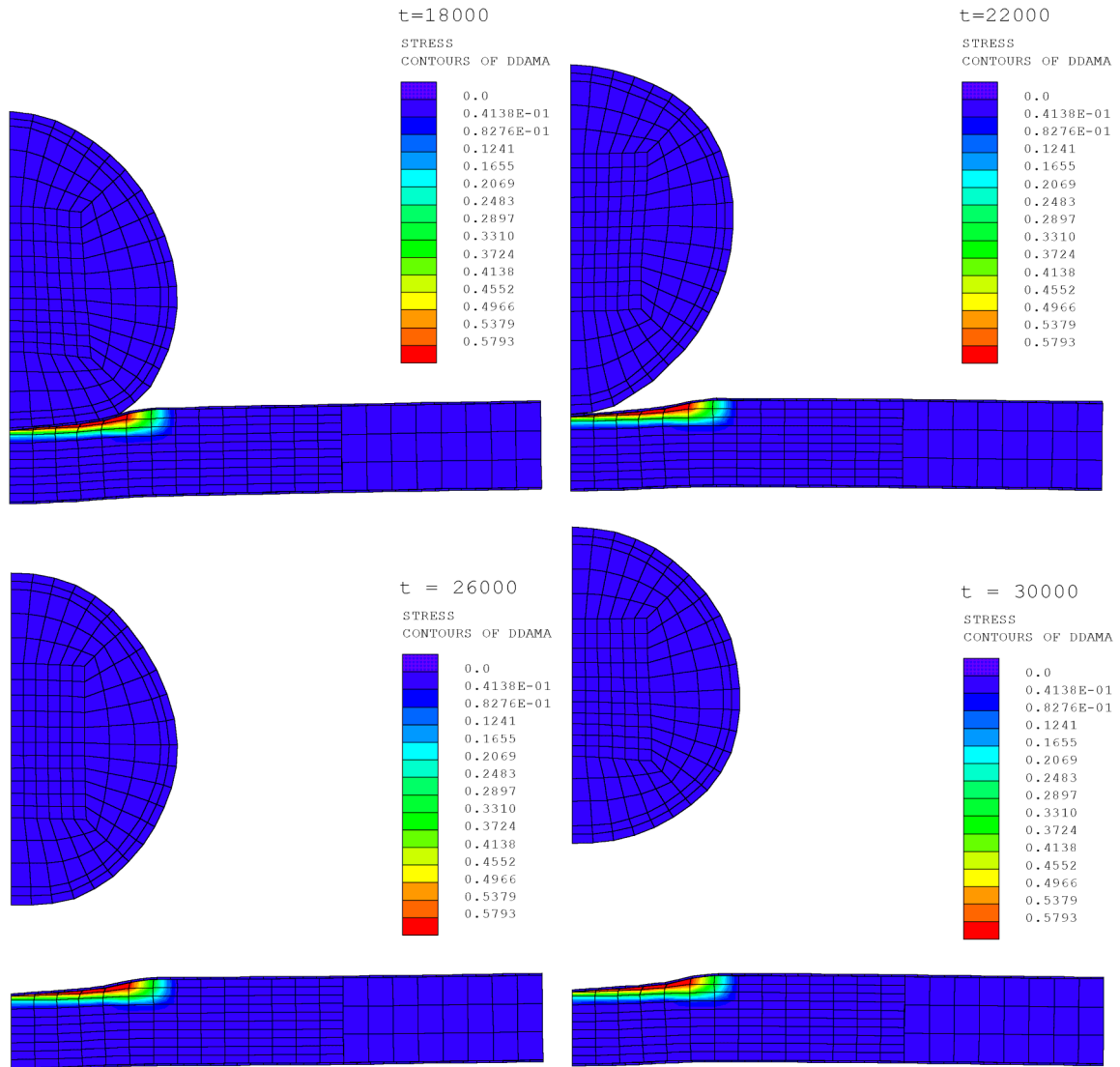
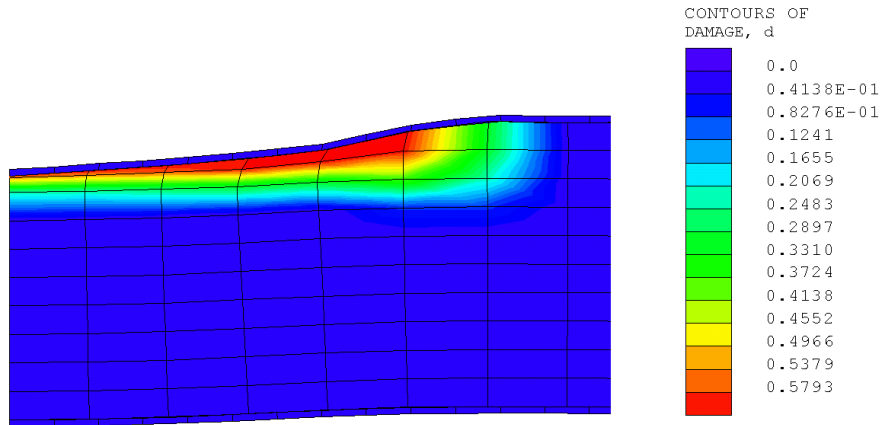


Figure 7b - Soft impact model response steps 5 to 8

During the impact event the soft body projectile deforms over the surface of the sandwich causing a shallow, large plan area, defect to remain in the sandwich. Accompanying this defect is a bulge on the reverse side of the sandwich. In fact, the reverse side bulge is seen in experimental testing. By examining the contours of damage d it is possible to estimate the extent of honeycomb crushing in the core of the sandwich. Figure 8 shows a detailed close-up of the impact region with the damage contours displayed. The distribution of the damage is located in a thin layer of constant depth below the skin of the contact. This closely resembles the damage obtained experimentally and illustrated in Figure 1. The physical dimensions of impact damage are detailed in Table 2 with comparisons to the experiments.


 Figure 8 - Close up of impact damage zone with contours of damage d .

Quantifying Parameter	Experimental	Model Prediction
Core damage diameter (internal)	115 mm	110 mm
Core damage depth (internal)	3.5 mm	3.7-5.1 mm
Permanent damage depth (external)	2.3 mm	4.8 mm

 Table 2 - Damage comparison for a normal impact velocity of 27.9 ms^{-1} .

The experimental impacts had an average impact diameter of 115mm. The damage predicted numerically is slightly smaller at 110mm. This variance can be attributed partly to the model of the soft body. In this instance the projectile does not quite deform to the same extent as its fluid filled experimental counterpart, reducing the contact area and correspondingly the damage diameter. A further source of error may be attributed to the numerical model being a continuum whereas the experimental material is a series of discrete units. This means that damage may progress at an even rate throughout the continuum when in the experimental case the damage occurs in cellular jumps of approximately 3mm at a time.

The depth of the core damage predicted by the numerical simulation is close to that of the experimental tests. The major issue is the upper and lower bounds for the depth of internal damage predicted by the numerical impact model. Outside the region of full honeycomb collapse ($d = 0.6$) there exists a gradient falling to $d = 0$ because the evolution occurred at a finite gradient, limited by numerical stability. The real damage boundary may be expected to lie in a position between the upper and lower bounds. Interpretation of the actual damage boundary from the model raises the issue of core damage as calculated by visual inspection of the experimental specimens. For the experimental case damage is quantified as the region containing elastic buckling. This equates to a step jump in the equivalent damage parameter across the visual boundary from 0 to 0.6. It is likely however that compression failure in the honeycomb core exists in a boundary around the major elastic buckling regions on a smaller scale similar to the gradient boundary.

The external damage volume predicted by the numerical model over-estimates the permanent deformation by a factor of two. This is partly related to relaxation that the defect

region undergoes after impact and also sectioning of the experimental panels. However, the model has the advantage that it can predict the maximum indentation due to the impact. The bulge on the reverse back face of the honeycomb sandwich that develops in the numerical simulation is seen in the experimental specimens.

The second numerical simulation analysed is the response of the sandwich to a “rigid” impact. The impactor has a Young’s modulus of 15GPa. The velocity of the projectile is reduced to 15.3ms^{-1} normal to the sandwich surface. Along with the velocity the projectile density is also reduced to 825kg/m^3 giving an effective impactor mass of 142 grams (impactor diameter of 69mm). Figure 9 illustrates the rigid body simulation after 28000 time increments, a total elapsed time of 2.4ms.

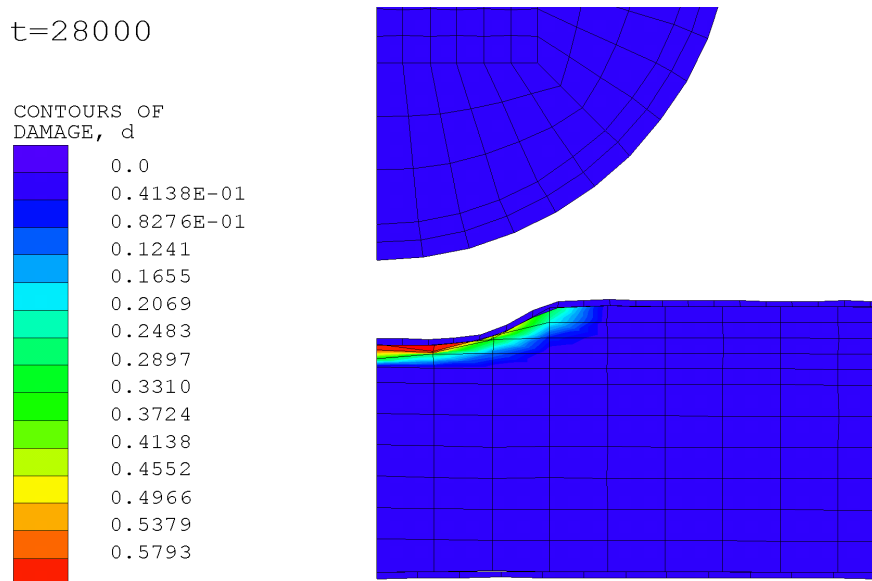


Figure 9 - Rigid body impact model damage.

The computed damage is best viewed in conjunction with Figure 2. The damage shown in the figure is an experimental panel, impacted by the rigid body described above. The boundary of the core crushing is depicted by arrows whilst the circled area represents the left boundary of the core damage. Considerable defect recovery has taken place in the figure of which a large component occurs as a result of sectioning the defect. A summary of the rigid impact tests is presented in Table 3.

Quantifying Parameter	Experimental	Model Prediction
Core damage diameter (internal)	55 mm	44 mm
Core damage depth (internal)	3.7 mm	4.5 - 5.5 mm
Permanent damage depth (external)	0.7 mm	3 mm

Table 3 - Rigid body impact damage comparison. (impact velocity = 15.3ms^{-1})

The numerical model appears to under estimate the width of core damage. This under estimate occurs because the model does not sufficiently calculate low level core damage in a thin layer at the defect boundary that occurs in the experimental case. A component of the lower numerical estimate may also be attributed once again to differences in modelling the damage formation in a continuum as opposed to a cellular structure that exhibits discrete 3mm jumps in the size of damage. In this instance the damage is underestimated by approximately three cell diameters.

Concluding Remarks

A model for non-metallic core crushing has been proposed based upon a combination of elastic, continuum damage and inelastic strain accumulation. The model has been incorporated into LUSAS [9]. Comparisons are made between the model and experimental impacts and the following conclusions can be drawn from this work:

- It is shown that a soft, compliant body impacting a Nomex core sandwich causes shallow crushing of the core. In comparison, hard uncompliant bodies impacting the same sandwich cause deeper damage that closely follows the shape of the projectile.
- A model has been proposed and incorporated into the LUSAS finite element package. Analysis of soft impacts using this model show good correlation with experimental panels in terms of the damage diameter and core crushing depth. The permanent deformation calculated by the model is about twice experimental for the panels impacted. This is due to a combination of time dependant recovery and also the sectioning of the experimental panels to make measurements. It is an estimate of the maximum deformation in the panel at peak impact.
- The model was used to simulate an impact by a hard body. The model predicted the behaviour of the hard impact to a reasonable degree with a slightly smaller predicted damage area but again greater permanent deformation.
- The material properties computed from static testing give a good estimate of the values required for the impact model. The use of a damage truncation level (d_{max}) in the damage model allowed good prediction of the likely damage depth.
- The linear damage evolution function good numerical stability even at relatively high gradients. The damage was allowed to evolve in conjunction with the inelastic strains that also added to the numerical stability of the process.

References

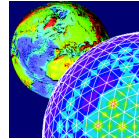
1. Minguet, P.J. (1991). A Model for Predicting the Behaviour of Impact Damaged Minimum Gage Sandwich Panels Under Compression. J. AIAA 91-1075-CP pp1112-1122.
2. Chang, F.K., Choi, H.Y. and Wang, H.S. (1990). Damage of Laminated Composites Due to Low Velocity Impact. Proceedings of the 31st AIAA/ASME/ASCE/AHS/ASC Structures, Structural Dynamics and Materials Conference, Long Beach, CA.

3. Kassapoglou, C. and Abbott, R. (1988). A Correlation Parameter for Predicting the Compressive Strength of Composite Sandwich Panels After Low Speed Impact. Proceedings 29th AIAA/ASME/ASCE/AHS/ASC Structures, Structural Dynamics and Materials Conference, Williamsburg VA.
4. Wierzbicki, T., Alvarez, A. and Hoo Fatt, M.S. (1995). Impact Energy Absorption of Sandwich Plates with Crushable Core. ASME AMD 205 Impact, Waves and Fracture pp391-411.
5. Aitken, R., Horrigan, D. and Moltschaniwskyj, G., Impacting Thin Skinned Composite Sandwich Laminates, Proceedings of 19th Symposium of the International Committee on Aeronautical Fatigue, 18-20 June 1997, Edinburgh, Scotland.
6. Ashby, M.F. and Gibson, L.J. (1988). Cellular Solids – Structure and Properties. Pergamon Press.
7. LUSAS Theory Manual Part 1. FEA Ltd., Kingston Upon Thames, Surrey, UK.

Contact Information

D.P.W. Horrigan

Email: d.horrigan@auckland.ac.nz



FEA Ltd
Forge House
66 High Street
Kingston upon Thames
Surrey, KT1 1HN, UK.

Tel: +44 (0)20 8541 1999
Fax: +44 (0)20 8549 9399
Email: info@lusas.com
<http://www.lusas.com>

